THE ASTROPHYSICAL JOURNAL, 345:759–769, 1989 October 15

VELOCITIES OF STARS IN REMOTE GALACTIC SATELLITES AND THE MASS OF THE GALAXY[1]

DENNIS ZARITSKY AND EDWARD W. OLSZEWSKI
Steward Observatory, University of Arizona
ROBERT A. SCHOMMER
Rutgers University
RUTH C. PETERSON
Whipple Observatory, Smithsonian Astrophysical Observatory
AND
MARC AARONSON[2]
Steward Observatory, University of Arizona
Received 1988 December 19; accepted 1989 April 8

ABSTRACT

We present observations of stars in four distant satellites of our Galaxy, Eridanus, Palomar 14, Leo I, and Leo II. From these data we derive, using a technique of wavelength calibration which utilizes an etalon, the heliocentric systemic velocities of these systems, -21 ± 4, 72 ± 4, 285 ± 3, and 70 ± 4 km s^{-1}, respectively. The value of the velocity for Leo I is in significant disagreement with previously published values. These systems are added to the remote satellite data base from which we estimate the mass of the Galaxy using a statistical method as well as timing arguments. The mass derived using the statistical techniques is $9.3^{+4.1}_{-1.2} \times 10^{11}\ M_\odot$ assuming radial satellite orbits, and $12.5^{+8.4}_{-3.2} \times 10^{11}\ M_\odot$ assuming isotropic satellite orbits. A lower mass limit, $13 \times 10^{11}\ M_\odot$, was derived from timing arguments, for an age of the universe of 1.4×10^{10} yr and for the accepted Galactocentric distance of Leo I, and can change by at most 25% for reasonable changes to the input parameters. These values are valid only if Leo I is gravitationally bound to the Galaxy, and we present arguments which support this assumption. We also use the data to acquire preliminary values of the internal velocity dispersions and mass-to-light ratios in Leo I and II.

Subject headings: galaxies: Local Group — galaxies: redshifts — galaxies: The Galaxy

I. INTRODUCTION

Over the past 20 years a compelling case has been made with observed neutral hydrogen rotation curves that some spiral galaxies possess massive dark matter halos (e.g. Bosma 1978; Rubin *et al.* 1982). Most of these rotation curves are flat or even rising over the entire observed range of radii, which implies the existence of a significant amount of mass at large radii, albeit not necessarily dark matter for all spirals (Kent 1988). Knowledge of the extent of, and mass in, dark halos is important to many areas of study involving extragalactic astronomy; for example, galaxy formation, gravitational lensing, galaxy cluster dynamics, and galaxy dynamics. Unfortunately, neutral hydrogen rotation curves cannot be measured to very large radii, $\sim$100 kpc, and as a result we know very little about the mass distribution at such radii. Studies of binary galaxies confirm the large mass-to-light ratios inferred from the flat rotation curves, although these studies suffer from difficulties in the analysis (White *et al.* 1983; Schweizer 1987). The question regarding the extent of dark matter halos in isolated galaxies remains relatively unaddressed observationally, except for the case of the Milky Way galaxy.

The remote satellites of our galaxy provide an invaluable tool for measuring the mass and extent of the dark matter halo out to radii of 200 kpc. Previous studies by Hartwick and Sargent (1978), Lynden-Bell, Cannon, and Godwin (1983, hereafter LCG), Peterson (1985), Olszewski, Peterson, and Aaronson (1986, hereafter OPA), Little and Tremaine (1987, hereafter LT), and Peterson and Latham (1989, hereafter PL) presented radial velocity measurements for some of the farthest satellites, either globular clusters or dwarf spheroidal galaxies, and also presented a variety of analysis techniques with which to estimate the mass of the Galaxy. The latest substantial increase to the data base was presented by OPA who concluded that the mass of the Galaxy, M_G, is $(5 \pm 2) \times 10^{11}\ M_\odot$, if the velocities of the satellites are distributed isotropically. LT developed a more sophisticated mathematical treatment of the problem based on a statistical analysis technique that enabled them to quantify the uncertainties in the mass determination. Using the data presented by OPA, they concluded that $M_G = 2.4^{+1.3}_{-0.7} \times 10^{11}\ M_\odot$[3] for isotropically distributed satellite velocities. LT excluded some satellites from their preferred sample because of uncertainties in the measured velocities; however, the results from these studies are in agreement, within the quoted errors, despite this exclusion. Uncertainties in the measured velocities were large for some of the remote systems, in particular Eridanus, Pal 14, Leo I, and Leo II. Since the farthest systems place the most rigid constraints, velocities for Leo I and Leo II are possibly critical in estimating the mass of the Galaxy and the properties of the halo.

[1] Observations reported here were obtained at the Multiple Mirror Telescope Observatory, a joint facility of the University of Arizona and the Smithsonian Institution.

[2] Deceased 1987 April 30.

[3] Except in this case for which the quoted error represents the 60% confidence level as given by LT, all quoted errors on statistically determined mass estimates represent the 90% confidence level.

The measured velocities of stars in two remote satellites, Draco and Ursa Minor, provide strong evidence for large amounts of dark matter *interior* to these systems (Aaronson 1983; Aaronson and Olszewski 1988). All of the dwarf spheroidals, except Leo I and Leo II which are the farthest, have had multiple member stars observed and therefore have estimated velocity dispersions (for Fornax see Seitzer and Frogel 1985; for Sculptor see Armandroff and DaCosta 1986; for Carina see Godwin and Lynden-Bell 1987 and Aaronson and Olzewski 1988). Draco and Ursa Minor are the most thoroughly studied and the only two which show evidence for copious amounts of dark matter at radii smaller than the core radius, r_c. This does not preclude large amounts of dark matter outside r_c for the other dwarf spheroidals. For the sample of the five dwarf spheroidals for which mass-to-light ratios, M/L, are available, M/L apparently varies inversely with the luminosity of the system. It is of interest to enlarge the sample and test this conclusion because the presence of dark matter has important implications for the formation and evolution of these systems.

We present observations of red giant stars in Eridanus and Pal 14, which are distant globular clusters, and of carbon stars in Leo I and Leo II. Some of the spectra were wavelength-calibrated with a technique which utilizes an etalon and enables one to calibrate precisely and uniformly across the spectrum. This technique and the observations are described in § II. Our results for the mass of the Galaxy and for M/L for Leo I and II are presented in § III.

II. OBSERVATIONS

The data were taken at the Multiple Mirror Telescope (MMT), with the MMT spectrograph utilizing either the 600 line mm^{-1} grating in second order, which we shall refer to as the low-resolution mode, or the echellette grating in 11th order (with a filter which blocks light from other orders), which we shall refer to as the high-resolution mode, and the dual-channel intensified Reticon detector, which records spectra from two 2".5 apertures separated by 36" on the sky. The spectral coverage in the low-resolution mode was approximately from 4700 Å to 6000 Å with a resolution of 1.3 Å. The spectral coverage in the high-resolution mode was approximately from 5200 Å to 5600 Å, for the central portion of the order, with a resolution of 0.6 Å. The data are from observing runs during 1986 January, February, March, and September, and 1988 January and March, predominantly in the low-resolution mode. The Pal 14 data, which are from 1988 March, were reduced independently in the manner described by Peterson and Foltz (1986).

Observing techniques varied slightly from run to run. Beam-switching, alternately observing the object through the right and then the left channel in subsequent exposures, was used only in the 1986 January and 1988 January runs. Typical exposure times for program objects were 900 s with no beam switching and 450 s per channel when beam switching was used. Comparison lamp spectra, and etalon spectra for the low-resolution observations, were taken before and after each object exposure, or pair of exposures when beam-switching was used, during all the runs. Several exposures were eventually combined to produce the final object spectra.

The data were reduced using NOAO IRAF[4] Version 2.7 on a Sun 4 computer at Steward Observatory. The spectra were flat-fielded by dividing them by a spectrum of an incandescent lamp, observed through the corresponding channel, which had the continuum component removed. This procedure removed pixel-to-pixel sensitivity variations in the Reticon detectors. We note that the data from each channel were independently reduced and combined with the data from the other channel only after the wavelength calibration was complete.

For accurate wavelength calibration, a large number of strong lines distributed through the entire spectral range is essential. In the low-resolution mode none of the three comparison lamps available for wavelength calibration, HgCd, FeNe and HeAr, has a sufficient number of lines of adequate brightness in the central region of the spectral range, 5100 Å to 5800 Å; therefore, wavelength calibration with comparison lamps is untrustworthy in that region. The lamps do have useful lines outside this area (see Fig. 1*a*). This fact, and the fact that we wished to measure velocities of C stars by using spectra in the region of the λ5363 C_2 Swan band, motivated the use of the etalon for wavelength calibration. The presence of strong lines in both edges of the calibration lamp spectrum is a necessary condition for the application of this calibration technique.

The etalon is simply a Fabry-Perot interferometer for which the gap distance is not tunable. It consists of two parallel, partially transmitting mirrors separated by an air gap and illuminated by collimated white light. Light with wavelengths commensurate with the interplate spacing will interfere and produce the pattern seen in the spectrum of transmitted light shown in Figure 1*b* (for more detail about etalons see Hernandez 1986 and for more detail about the MMT etalon in particular see Foltz *et al.* 1985).

A pair of neighboring comparison lamp and etalon exposures was chosen at random from the data of the particular night being reduced. The lines in the ArCdFeHeHgNe lamp spectra were identified and used to derive the wavelength solution that was then applied to the etalon spectra. This wavelength solution typically consisted of five third-order splines, used approximately 20 lines, and had an rms error of $\approx$0.2 Å. Since most of the calibration lamp's spectral lines are at the edges, the wavelength solution is good at the edges but poor in the middle. The wavelengths of all the lines in the etalon spectra were then measured.

The wavelength of a particular line (e.g., fringe) produced by an etalon is given by

$$\lambda = C/n\,, \tag{1}$$

where C is a constant that contains information on the viewing angle, interplate spacing, and refraction indices, and n is the order number of the line in question. The value of n for a given line is not necessarily an integer, since the multilayer coatings of the etalon produce phase shifts during reflection. We made the assumption that the difference in order number between neighboring lines, Δn, was 1. The dependence of the characteristics of the multilayer dielectric coating on wavelength could in practice produce a nonnegligible effect on Δn and cause Δn to be slightly different than 1. The only justification for our assumption that this effect was unimportant is the high precision of the wavelength solutions subsequently attained. Using all the etalon lines from regions of the spectra where the wavelength calibration from the ArCdFeHeHgNe lamp is accurate, a best-fit n for a given spectral line and C were derived. We then produced a line list for the etalon spectrum by using equation (1). This list was subsequently used to identify the lines in the uncalibrated etalon spectrum, and we then derived

[4] IRAF is distributed by the National Optical Observatories, which is operated by AURA, Inc., under contract to the NSF.

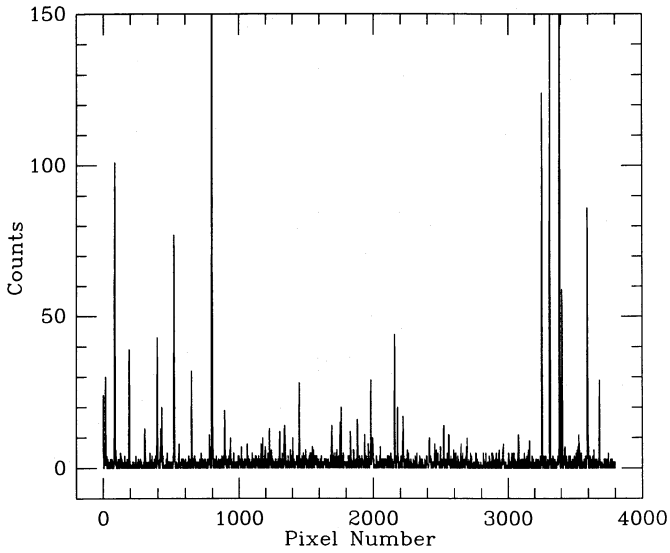

FIG. 1*a*

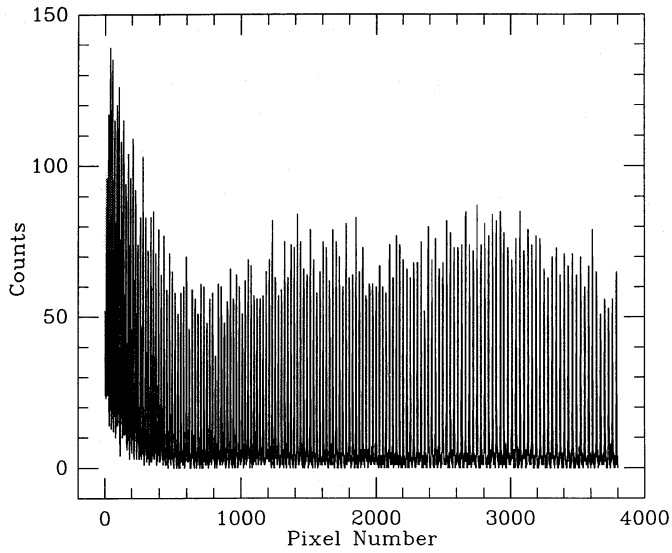

FIG. 1*b*

FIG. 1.—(*a*) The spectra of the combination of HeAr, FeNe, and HgCd lamps from a 120 s exposure. Line centering is only sufficiently precise for lines with more than ~20 counts. The majority of lines seen in the central portion of the spectrum are third-order lines which have leaked through the filter. There are roughly 20 usable lines in this spectrum. (*b*) The spectra of the transmitted light through the etlon from a 60 s exposure. There are roughly 140 usable lines in this spectrum.

a wavelength solution by fitting a high-order (≈15) Chebyshev polynomial to approximately 140 lines. The wavelength solution had an rms error of 0.15 Å to 0.2 Å. This rms error is only slightly less than that of the wavelength solution from the calibration lamp; however, the advantage of this technique is that the entire spectrum is calibrated with this precision since the spacing between adjacent spectral lines is 7 to 10 Å.

This "identified" etalon spectrum was then used to identify the spectral lines in other etalon spectra taken that night. If conditions are stable, C will remain constant through the night and the wavelengths of the lines will remain the same. We used the IRAF "noao.onedspec.reidentify" command cautiously to match the corresponding lines in other etalon spectra from the same night to those in the "identified" spectrum. The wavelength solutions were then reevaluated. The process was repeated for each night independently. This technique worked well for the large majority of etalon spectra. However, there were two occasional failure modes, the first of which was due to large flexure in the spectrograph. If the spectral lines were shifted by a significant portion of the interval separating adjacent lines, the reidentification of lines became ambiguous. The second failure mode was probably due to changes in the temperature or humidity. These changes cause a corresponding change in C; therefore, the wavelengths in the line list are incorrect and the calibration fails. This became most noticeable for the data taken at the beginning and end of nights when the temperature might have been undergoing large changes. Whichever the cause of the failure, the etalon spectrum was recalibrated with calibration lamps taken immediately before or after that particular etalon exposure and the problem was corrected.

The high-resolution data were calibrated with the available calibration lamps. However, we had to limit ourselves to the spectral region between 5400 Å and 5600 Å because this was the only region with a sufficient number of strong lines for precise wavelength calibration. The wavelength solution used consisted of a medium order (~6) Chebyshev polynomial which was fitted to approximately 15 lines and had an associated rms error of ≈0.05 Å.

Velocities were measured using a cross-correlation program based on the algorithm described by Tonry and Davis (1979). M3 AA was used as the velocity template for the high-resolution data. Both HD 77234 and HD 76846 were used as carbon star velocity templates. The template which produced the larger correlation peak for a given program carbon star was used for that object. The spectrum of the star NGC 1904–300 was used as the giant star velocity template for the low-resolution giant star spectra. The results from this analysis are presented in Tables 1 and 2 (Table 1 also contains references to the names of the standard stars and to their velocities). Velocities were accepted only if the correlation peak was at least 2.5 times stronger than the largest noise peak.

Observational uncertainties were estimated from our measurements of standard star velocities (cf. Table 1) and from multiple observations of program objects. The velocities obtained from the low-resolution mode standard star spectra indicate that the standard deviation of a single measurement in this mode is 7 km s^{-1}; therefore, we were able to achieve errors of approximately 1/10th of a resolution element using the etalon wavelength calibration technique. This result justifies our assumption that $\Delta n = 1$. Although the standard star spectra have a much larger signal-to-noise ratio (S/N) than the program objects, the uncertainties in the derived velocities for the program objects do not appear to be much larger. The standard deviation among the velocities for stars with multiple measurements is 8 km s^{-1}, which is in acceptable agreement with the uncertainty derived from observations of standard stars. We stress that this includes any internal velocity dispersion in these systems; however, we have adopted 8 km s^{-1} as the single measurement velocity uncertainty. We feel that with greater S/N in the etalon exposures, with spline-fitting routines that are optimized for the etalon wavelength calibration technique, and with shorter object exposures (flexure during the exposure is not neglible for the longer exposures) wavelength

TABLE 1

MEASURED HELIOCENTRIC VELOCITIES FOR STANDARD STARS

Object	Measured v (km s^{-1})	Standard v (km s^{-1})
Low-Resolution Mode		
HD 156074[a]	−20	−12.5
HD 30443[a]	65	68
HD 32963[b]	−56	−63
HD 76846[a]	31, 26, 19, 31	24.6
HD 77234[a]	14, 8, 10, 7	7.3
M3 AA[c]	−151	−148
NGC 1904–241[d]	224	209
NGC 1904–300[e]	200	211
NGC 288–20C[d]	−52	−48
High-Resolution Mode		
HD 112299[b]	4	3.8
M3 AA[c]	−148	−148
M5 IV 34[d]	56	51.0
M15 K825[d]	−104	−96
M67 F170[e]	35	34.3
M67 S 995[e]	31	33.3
NGC 288–20C[d]	−47, −51	−48
NGC 1904–15[d]	208, 196, 207, 206	207
NGC 1904–241[d]	210, 204, 210, 211	209
NGC 1904–300[d]	210, 212, 212	211
NGC 4147 II 30[d]	182	183.5
NGC 4388[b]	−30	−28
NGC 5053 E[f]	40	43.4
NGC 5053 L[f]	44	43.7
NGC 5053–72[f]	37	43.3
NGC 6366 II 70[g]	−119	−122.6
NGC 6366 III 8[g]	−120	−122
NGC 6366 III 55[g,h]	−118	−119.5
		−122.4

[a] Carbon star; velocities are from private communication from R. McClure to M. A. several years ago, and from numerous measurements by E. W. O. and M. A. using the MMT echelle.

[b] F–K stars; velocities quoted are from *Transactions of the IAU*, Vol. **15A**, p. 409 (1973) and from numerous measurements by E. W. O. and M. A. using the MMT echelle.

[c] M3 AA = VZ 238; velocities from Pryor, Latham, and Hazen (1988) and a similar number of measurements by M. A. and E. W. O. using the MMT echelle.

[d] See Table 1 in Peterson, Olszewski, and Aaronson (1986) for velocities and star identifications; E. W. O. has also made follow-up measurements of the velocities of these stars using the MMT echelle.

[e] Velocities from Mathieu *et al.* 1986.

[f] Velocities are from multiple unpublished MMT echelle measurements by E. W. O., C. Pryor, and R. A. S. Star identifications from Sandage, Katem, and Johnson (1977).

[g] Velocities from single MMT echelle measurements by E. W. O. Star identifications from Pike 1976.

[h] Velocities from Da Costa and Seitzer 1989.

calibration and velocities could be further improved. The velocities obtained from the high-resolution standard star spectra indicate that the velocity errors for stars in this data set is 4 km s^{-1}. This is again approximately equivalent to 1/10th of a resolution element. For Pal 14 HS 54, which has lower S/N, the error increases to 7 km s^{-1}.

III. RESULTS AND DISCUSSION

In Table 2 we present our measurements of the heliocentric velocities of stars in Leo I, Leo II, Eridanus, and Pal 14. The systemic velocity of a particular system is an average of the observed velocities of stars in that system and the associated error is the standard deviation of the mean. The systemic

TABLE 2

MEASURED HELIOCENTRIC VELOCITIES FOR PROGRAM STARS[a]

Star	v (km s^{-1})
Leo I[b]	
ALW 2	289 (1986 Feb), 267 (1986 Mar)
ALW 5	291 (1988 Jan), 289 (1986 Feb), 273 (1986 Mar)
ALW 7	288 (1986 Feb)
ALW 14	292 (1986 Feb), 303 (1988 Jan)
ALW 15	286 (1986 Feb)
ALW 20	280 (1986 Mar)
Leo II[c]	
ALW 1	59 (1986 Jan)
ALW 3	68 (1986 Feb), 56 (1988 Jan)
ALW 4	73 (1986 Jan)
ALW 5	82 (1986 Jan)
ALW 6	67 (1986 Feb), 78 (1988 Jan)
Eridanus[d] and Pal 14[e]	
Eridanus 25	−20 (1988 Jan)
Eridanus 26	−22 (1988 Jan)
Eridanus 27	−21 (1986 Sep)
Pal 14 HS 54	67 (1988 Mar)

[a] Date of observation follows value in parenthesis.

[b] Although some of these stars in Leo I were discovered independently by E. W. O. and M. A., since the charts by Azzopardi, Lequeux, and Westerlund (1985 and 1986) have been published we refer to them by their ALW names. Data from low resolution mode.

[c] For convenience we also use the numbering scheme of Azzopardi, Lequeux, and Westerlund 1985. These stars were independently confirmed by M. A. and E. W. O. as C stars from candidates supplied by R. A. S. Data from low resolution mode.

[d] Identification from DaCosta 1985. Data for Eri 25 and 26 from low-resolution mode and data for Eri 27 from high-resolution mode.

[e] Identification from Hartwick and Sargent 1978. Data from high-resolution mode.

velocity of Pal 14, 72 ± 4 km s^{-1}, is a weighted average of the velocity for the star we observed, HS 54, and the velocity presented by OPA for HS 24, 73 ± 4 km s^{-1}. Our measurement of the systemic velocity of Leo II based on five stars, 70 ± 4 km s^{-1}, is in agreement, to within the errors, with the previously published value, 95 ± 25 km s^{-1} (Suntzeff *et al.* 1986). The result for Eridanus based on three stars, −21 ± 4 km s^{-1}, also confirms one of the previously published values, −20 ± 5 km s^{-1} (OPA). However, our result for Leo I based on six stars, 285 ± 3 km s^{-1}, is in significant disagreement with the previously published value, 185 ± 25 km s^{-1} (Suntzeff *et al.* 1986). The previous Leo I observations were at roughly 10 times lower resolution and therefore have random errors which are approximately 10 times greater; in addition, the quoted error does not represent possible systematic errors present in low-resolution velocity work.

To obtain Galactocentric velocities we converted from heliocentric velocities to local standard of rest (LSR) velocities by using a peculiar solar motion of 16.5 km s^{-1} toward $(l, b)^{II} = (53°, 25°)$, or in u, v, w notation (−9, 12, 7) km s^{-1} (Delhaye 1965). We then corrected for the rotation of the LSR about the center of the Galaxy using 220 km s^{-1} for the circular rotation speed at the radius of the Sun, and using for our displacement from the center of the Galaxy 6.8 kpc (Frenk and White 1982). The Galactocentric velocities and distances for all the remote systems are listed in Table 3. Leo I's large Galacto-

TABLE 3

VELOCITIES AND DISTANCES OF REMOTE SATELLITES OF THE MILKY WAY[a]

Object	$v_\odot$ (km s^{-1})	$\Delta v_\odot$ (km s^{-1})	v (km s^{-1})	Reference	r (kpc)	Reference
Pal 15[b]	69	1	148	1	36	9
LMC + SMC ...	245	5	61	2	51	10
Ursa Minor	−249	1	−88	3	65	11
Pal 14	72	4	166	4	75	12, 13
Draco	−289	1	−95	3	75	14
Sculptor	107	2	74	5	79	15
Eridanus	−21	4	−138	4	85	16
Carina	230	1	14	6	93	17
Pal 3	89	9	−59	7	95	18
NGC 2419	−20	5	−26	7	98	19
Pal 4	75	5	54	7	108	20
AM-1	116	15	−42	8	117	21
Fornax	55	5	−34	3	140	22
Leo II	70	4	16	4	220	23, 24
Leo I	285	2	177	4	230	23, 25

[a] Velocity, v, and distance, r, are Galactocentric.

[b] The distance of Pal 15 is not well determined due to the possibility of galactic absorption (Seitzer and Carney 1988). To be conservative, we adopt the smaller distance for the galactic mass analysis.

REFERENCES.—(1) PL. (2) Yahil, Tammann, and Sandage 1977. (3) Aaronson and Olszewski 1988. (4) This paper. (5) Armandroff and Da Costa 1986. (6) Cook, Schechter, and Aaronson 1983. (7) OPA. (8) Suntzeff, Olszewski, and Stetson 1985. (9) Seitzer and Carney 1988. (10) Schommer, Olszewski, and Aaronson 1984. (11) Olszewski and Aaronson 1985. (12) Harris and van den Bergh 1984. (13) Da Costa, Ortolani, and Mould 1982. (14) Stetson 1979. (15) Da Costa 1984. (16) Da Costa 1985. (17) Mould and Aaronson 1983. (18) Gratton and Ortolani 1984. (19) Racine and Harris 1975. (20) Christian and Heasley 1986. (21) Aaronson, Schommer, and Olszewski 1984. (22) Buonnano *et al.* 1985. (23) Hodge 1971. (24) Demers and Harris 1983. (25) Fox and Pritchet 1987.

centric radial velocity and distance make it invaluable for placing limits on the mass of the Galaxy.

a) Statistical Analysis

We begin our analysis by applying a technique developed by LT. Briefly, the technique evaluates the probability that the values of the quantity $v^2r/G(\equiv\mu)$ observed for the outer satellites would have been found for a given Galactic point mass potential, $\Phi = -GM/r$. This probability is expressed as $P(\mu\,|\,M)$. The desired quantity is $P(M\,|\,\mu)$, which one can evaluate by knowing $P(\mu\,|\,M)$, $P(M)$ and applying Bayes's theorem. $P(\mu\,|\,M)$ is evaluated assuming either isotropic or radial orbits for the satellites and no selection effects, of either an observational or physical nature. The recommended choice for $P(M)$ when the variable in question, in this case M, can vary from 0 to ∞, and when no other information is available, is $P(M) \propto M^{-1}$, although $P(M) \propto constant$ is also a reasonable choice. As LT demonstrated, using $P(M) \propto constant$ increases the derived mass by less than 25% for the sample they used. Since the effects for our larger sample should be smaller, since adopting $P(M) \propto M^{-1}$ is recommended, and since it produces the lower, more conservative, mass estimates, we adopted $P(M) \propto M^{-1}$. LT also presented an analysis which models the Galactic halo potential as that from an isothermal sphere, $\Phi = v_c^2 \ln(r)$. In this case, the desired probability is $P(v_c^2\,|\,v_r^2)$, which is the probability of having a halo with circular velocity v_c, if the observed radial velocity of the satellite is v_r. Analogously, we adopted $P(v_c^2) \propto v_c^{-2}$. Unfortunately, when Little and Tremaine did their analysis, precise and accurate velocities were not available for some of the distant satellites, including the two farthest satellites, Leo I and Leo II. The distant satellites are the most appropriate for the point mass approximation to the mass of the Galaxy and are also critical if one wants to contain all the mass of the galaxy interior to the orbit of the satellite. We present results from analyses with radial or isotropic orbits, with a point mass or isothermal sphere Galactic mass distribution, and with the enlarged data base.

The data used in the analysis is presented in Table 3. All the systems have Galactocentric distances greater than 50 kpc, except for Pal 15. We included it because although the most recent determination of the distance places it closer than 50 kpc (Seitzer and Carney 1988) it has historically been thought to be substantially farther away (e.g., Webbink 1985). The value we have adopted for the distance (from Seitzer and Carney 1988) is the most conservative one in the framework of our analysis. We have added from our own observations the velocities of Eridanus, Pal 14, Leo I, and Leo II to the data base and show the results from analyses done with and without Leo I (Fig. 2 and Table 4). Adding Pal 15 (from PL), Eridanus, Pal 14, and Leo II to LT's data set increases the mass of the Galaxy by a factor of 2. Assuming isotropically distributed satellite velocities, the median result, i.e., the value of M for which the probability that the mass of the Galaxy is larger than M is 50%, is $4.6 \times 10^{11}\ M_\odot$ [3.0×10^{11}, 8.5×10^{11}], where the values in brackets are the endpoints of the 90% confidence interval. This is to be compared with LT's preferred sample result of $2.4 \times 10^{11}\ M_\odot$ [1.4×10^{11}, 5.2×10^{11}]. With the increase of the median mass by over 90% the results now discriminate against the LT result at over the 90% confidence level. Adding Leo I to the analysis, again assuming isotropically distributed velocities, *further increases the estimated mass of the Galaxy by nearly a factor of 3* to $12.5 \times 10^{11}\ M_\odot$ [9.3×10^{11}, 20.9×10^{11}]. Including Leo I in the analysis produces a Galactic mass estimate of roughly $10^{12}\ M_\odot$ even with the assumption of radial satellite orbits.

The mass estimate resulting from the analysis of the sample including Leo I was previously discriminated against at the 99% confidence level. The LT probability analysis, while offering a statistically "robust" estimate of the Galactic mass and its associated confidence interval, is susceptible to some uncer-

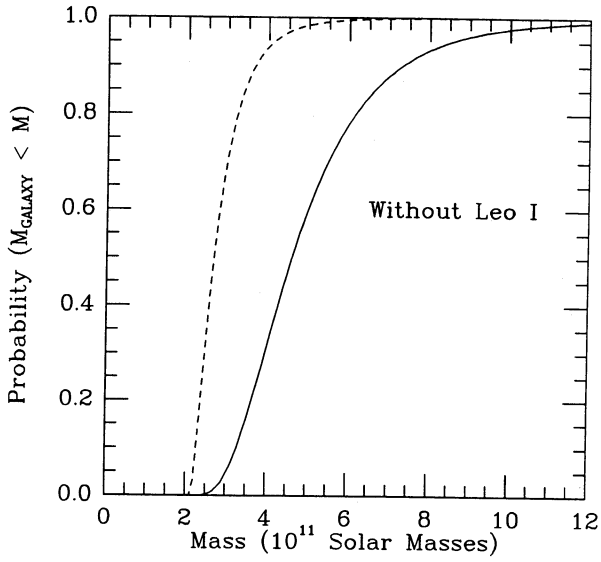

FIG. 2*a*

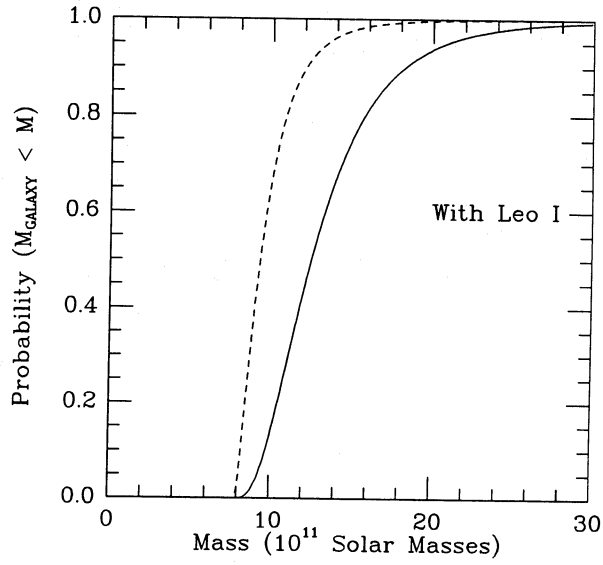

FIG. 2*b*

FIG. 2.—(*a*) The results from the statistical analysis using the satellite sample excluding Leo I. The dashed curve is from the analysis assuming radial satellite orbits and the solid line is from the analysis assuming isotropic orbits. (*b*) Same as (*a*) except the satellite sample includes Leo I.

tainties resulting from the small sample of satellites: in particular assumptions concerning the distribution of orbital eccentricities for satellites in the sample, and the form of the Galactic potential. In particular, one does not know the relationship between the parameter distribution of the known satellites and that of the adopted model family.

When the assumption of a point mass potential is replaced by an isothermal form for the potential, the results from the analysis for sets of satellites which include and exclude Leo I *are* in agreement within the errors (cf. Table 4). This agreement indicates that the isothermal sphere model may be a better representation of the halo than the point mass model. As shown graphically in Figure 3, the theoretical probability distribution from the isothermal sphere model for $\ln(v_r^2)$ is not inconsistent with the observed data distribution. The theoretical curve is independent of the assumption of isotropic or radial orbits. However, even if the model is valid and the derived characteristic velocity is correct, we cannot calculate the total Galactic mass because we do not know the extent of the halo.

The LT analysis presumes that the entire satellite population can be characterized by a single type of orbit family, i.e., radial or isotropic; however, little is known about the nature of the orbits of these remote satellites. The argument has been made that the outer satellites are not on circular orbits because they fail to lie in a plane (LT) and because galaxy collapse models lead to predominantly radial orbits (van Albada 1982; McGlynn 1984). However, circularization of orbits and tidal disruption are processes which could in principle decrease the eccentricities of the sample. Circularization of orbits by dynamical friction in the halo is pronounced for massive satellites, e.g., $M = 0.1\ M_G$ (Bontekoe and van Albada 1987). However, it is proportionally less important for the less massive satellites, which are under consideration here. LCG suggested that the eccentricity of the sample is smaller now than it was in the past because satellites on eccentric orbits pass close to the center of the Galaxy and suffer tidal disruption. Recent work (Allen and Richstone 1988; Zaritsky and White 1989) suggests that for objects on highly radial orbits the classical tidal radius formula significantly overestimates the effect of tidal stripping, primarily because of the relatively short time for which the satellite is near pericenter. However, it has been shown that bulge shocking during the early history of the Galaxy could "significantly alter the observed kinematics of the surviving population" (Aguilar, Hut, and Ostriker 1988). To complicate matters further, the magnitude of the effects discussed above may depend on Galactocentric distance; for example, tidal disruption might be more effective for inner satellites which by definition spend more time nearer to the center of the Galaxy. If one accepts this, one might expect that satellites would have different orbital characteristics as a function of mean Galactocentric distance. All these effects conspire to make the situation quite uncertain. Because we do not know the initial conditions of this system or the current space velo-

TABLE 4

RESULTS OF STATISTICAL (LT) ANALYSIS

SAMPLE	MASS OF THE GALAXY (Point Mass Model) ($10^{11}\ M_\odot$)		HALO CIRC. VELOCITY (Isothermal Sphere Model) (km s^{-1})	
	Radial Orbits	Isotropic Orbits	Radial Orbits	Isotropic Orbits
LT preferred sample (Sample 4)[a]	1.1 [0.8, 2.0]	2.3 [1.3, 5.0]	62 [45, 96]	107 [77, 165]
Entire sample excluding Leo I	2.7 [2.2, 4.1]	4.6 [3.0, 8.5]	89 [65, 128]	154 [115, 198]
Entire sample including Leo I	9.3 [8.1, 13.4]	12.5 [9.3, 20.9]	98 [73, 138]	169 [127, 237]

[a] These are our results for LT's preferred sample.

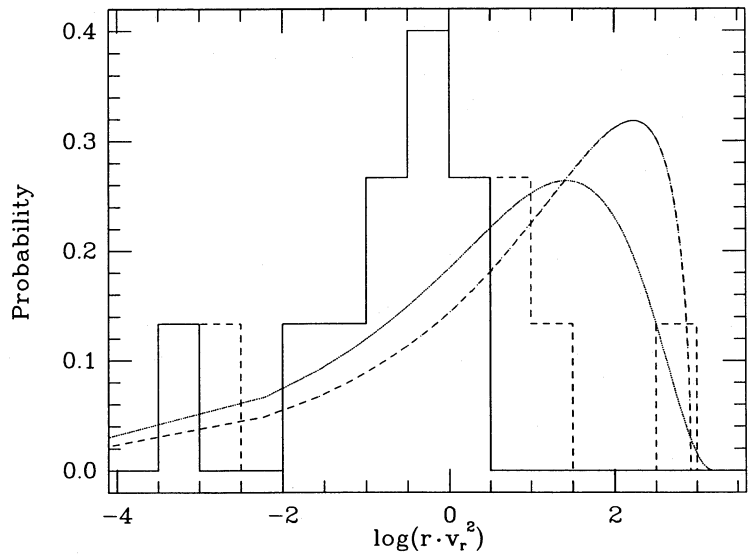

FIG. 3a

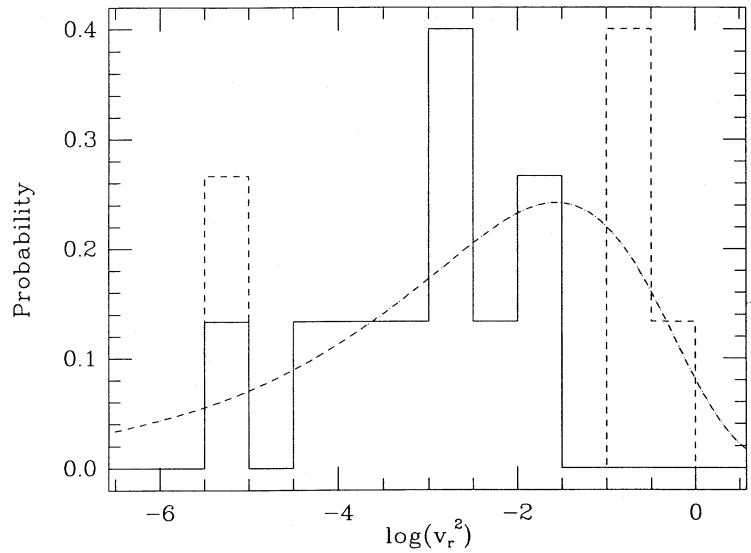

FIG. 3b

FIG. 3.—(*a*) We show the theoretical distribution of the natural logarithm of rv_r from the statistical models using the point mass Galactic potential and the observed distribution of the sample presented in Table 3. The dashed curve represents the distribution for radial orbits and the dotted curve the distribution for the isotropic orbits. The dashed portion of the histogram represents the data added by this study and PL. (*b*) We show the theoretical distribution of the natural logarithm of v_r^2 from the statistical models using the isothermal sphere Galactic potential and $v_c = 169$ for isotropic satellite orbits (*dotted line*) and the observed distribution of the sample presented in Table 3. The dashed line is also equivalently from the isothermal sphere model with radial satellite orbits and $v_c = 90$. The dashed portion of the histogram represents the data added by this study and PL.

cities of remote systems, the nature of the orbits of the outer satellites is not well determined.

The question of completeness is always a difficult one to quantify. The drastic change caused by the addition of principally one data point, Leo I, in the point mass models demonstrates an inherent weakness of any statistical analysis of this small data set. We therefore believe that the following timing arguments represent a more prudent approach to the derivation of the Milky Way's mass.

b) Timing Arguments

Leo I has an extreme velocity and distance among the satellites of our Galaxy. If it is gravitationally bound to the Milky Way, it is the key object in a mass analysis of the Galaxy because it can place an interesting lower limit on the total mass. Assuming that Leo I is bound, is on a purely radial orbit, and is *only* gravitationally influenced by the Milky Way, we recalculated, using basic timing arguments, the mass of the Galaxy. The fact that Leo I and M31 are separated by $\sim 115°$ on the sky makes the third assumption valid, at least to lowest order. To justify this assertion we examined the effect of including M31 using numerical simulations. The separation between M31 and the Galaxy was constrained to be greater than 300 kpc because of complexities which arise otherwise from the close interaction. Because the galaxies have spent the large majority of their lifetimes at large separation this simulation is relevant to the question at hand. We evaluated the time required in the various realizations for Leo I to travel between

TABLE 5

TIMING ARGUMENT MODELS

Model (1)	t (10^9 yr) (2)	v_c (km s^{-1}) (3)	$r_{\rm Leo}$ (kpc) (4)	$r_{\rm M31}$ (kpc) (5)	$v_{\rm Leo}$ (km s^{-1}) (6)	$v_{\rm M31}$ (km s^{-1}) (7)	M_G ($10^{11}\ M_\odot$) (8)	$M_{\rm LG}$ ($10^{11}\ M_\odot$) (9)	$M_{\rm M31+MW}$ ($10^{11}\ M_\odot$) (10)
1.....	10	220	230	710	178	−118	15	50	41
2.....	14	220	230	710	178	−118	13	38	36
3.....	18	220	230	710	178	−118	12	31	33
4.....	14	200	230	710	162	−108	11	34	30
5.....	14	240	230	710	194	−127	15	41	41
6.....	14	220	230	685	178	−118	13	35	36
7.....	14	220	150	710	178	−118	7	38	19
8.....	14	220	200	710	178	−118	11	38	30

two points in its orbit which are at the same distance from the Galaxy. The effect of increasing the mass of M31 from zero, as assumed in the following timing arguments, to $25 \times 10^{11}\ M_\odot$, which is the solution to the Local Group timing argument, is an increase of ~5% in the measured time. For comparison, a change of $1 \times 10^{11}\ M_\odot$ in the mass of the Galaxy, for mass estimates near the solution to the timing arguments, produces a 15% change in the measured time. Therefore, the omission of M31 in the analysis introduces a relatively small uncertainty and would appear on the basis of these simulations to *decrease* the estimated mass of the Galaxy. In addition, the results we present from timing arguments are *conservative* because of the first two assumptions and timing arguments have the advantage that generalizing assumptions concerning a set of data, e.g., radial orbits for all the satellites, do not have to be made.

Equations that describe the orbit of a test particle emitted radially at $t = 0$ and attracted by a mass M at the origin have been derived and used to estimate the mass of the Local Group (Kahn and Woltjer 1959; Sandage 1986). The description of the test particle's orbit is given by

$$r = \frac{GM}{-2E}(1 - \cos\theta) \tag{2}$$

and

$$t = \frac{GM}{(-2E)^{(3/2)}}(\theta - \sin\theta)\,, \tag{3}$$

which imply

$$v = \frac{GM}{(-2E)^{(1/2)}}\frac{\sin\theta}{r}\,, \tag{4}$$

where the "known" quantities are r, the present distance to the test particle; v, the radial velocity of the test particle; and t, the age of the universe; and the unknown quantities are M, the mass of the object to which the test particle is bound; E, the energy of the test particle; and θ, a parameter that describes the orbital position of the test particle. The equations can be rewritten to provide expressions for r, t, and M in terms of θ

$$r^3 = \frac{GMt^2(1 - \cos\theta)^3}{(\theta - \sin\theta)^2}\,, \tag{5}$$

$$\frac{r}{vt} = \frac{(1 - \cos\theta)^2}{\sin\theta(\theta - \sin\theta)}\,, \tag{6}$$

and

$$M = \frac{r^3}{t^2}\frac{(\theta - \sin\theta)^2}{(1 - \cos\theta)^3}\,. \tag{7}$$

These equations can be used for the Leo I–Milky Way system and for the M31–Milky Way system. Although the latter is not a case which can be described as a test particle system the above equations are valid if M31 and the Milky Way are bound to each other and on radial orbits. For the Leo I–Milky Way analysis M represents the mass of the Milky Way while for the M31–Milky Way analysis M represents the total Local Group mass, i.e. M31 + Milky Way. For both systems we present the solutions with the smallest value of θ, i.e., the minimum number of complete orbits. This also leads to the lowest possible mass estimates. The adopted solution for M31 and the Milky Way has the galaxies having passed their maximum separation for the first time. On the other hand, the adopted solution for Leo I and the Milky Way has the galaxies approaching their maximum separation for the second time. We stress that Leo I has not yet completed a single orbit, and it is therefore invalid to assume, as is done in the statistical analysis, that it has a random orbital phase.

We ran a variety of models to determine the range of the allowed Galactic mass and present the results for some of models in Table 5. In column (8) we present the mass of the Galaxy as given by the Leo I–Milky Way timing argument. In column (9) we present the mass of the Local Group as derived from the M31–Milky Way timing argument. In column (10) we present the mass of the Local Group as predicted by the Leo I–Milky Way timing argument assuming that the mass of the Local Group is concentrated entirely in M31 and the Milky Way and that M31 and the Milky Way have the same M/L value, and adopting −21.1 and −20.5 for the absolute magnitudes of M31 and the Milky Way, respectively (van den Bergh 1980).

The models show that for the preferred parameters, i.e., a distance of 710 kpc to M31 (Welch *et al.* 1986), a Galactocentric radial velocity of M31 of −118 km s^{-1} (Dean and Davies 1975), a Galactocentric distance of 230 kpc for Leo I (Hodge 1971; Fox and Prichet 1987), a Galactocentric velocity for Leo I of 177 km s^{-1} (this paper), and an age of the universe of 1.4×10^{10} yr (model 2), the agreement between the mass of the Local Group predicted from the application of the timing argument to Leo I and the Milky Way, and the mass of the Local Group predicted from the application of the timing argument to M31 and the Milky Way is remarkable. In models 4–5 we probe the sensitivity of the results to changes in the adopted Galactic rotation speed adopted for the LSR. Because of the geometry of the system, i.e., that the angle between the Galactocentric radius vectors to Leo I and M31 is 105° when projected onto the rotation plane of the Galaxy and that Leo I is moving away while M31 is moving toward the Galaxy, changes in the adopted circular velocity increase or decrease

the magnitude of both velocities, and therefore affect both mass estimates in the same sense. The final models examine the dependence of the estimated masses on the adopted distance to Leo I and to M31. The distance to Leo I is the worst determined quantity of all those required in this analysis. Model 7 demonstrates that to decrease the estimated mass of the Galaxy by a factor of 2 requires that the distance to Leo I be 150 kpc.[5]

We stress that the mass estimates from these timing arguments are lower limits because we have excluded the tangential components of the velocities of Leo I and M31 and because we treat the galaxies as point masses. A timing argument analysis of the Local Group which allows for a tangential component in the velocity of M31 is described by Einasto and Lynden-Bell (1982) and predictably gives somewhat larger masses than the purely radial models. The result from that analysis is that the mass of the Local Group is between 3 and $7 \times 10^{12}\ M_\odot$. However, the mass estimate for our galaxy which we present from the timing argument using Leo I is also a lower limit. Because of the uncertainties that this presents, it is not judicious to discriminate closely between models presented in Table 5. The agreement between the mass estimates from the Leo I and M31 timing arguments with the preferred input parameters, albeit without the inclusion of the tangential velocity components, is encouraging and removes the discrepancy between the previous mass estimates based on remote satellites (e.g., OPA and LT) and Local Group timing arguments. From this analysis we conclude that $M_G = (13 \pm 2) \times 10^{11}\ M_\odot$ if Leo I has a radial orbit. We note that for this Galactic mass and for a halo circular velocity of 170 km s^{-1}, which is approximately the result from the statistical analysis for isotropic satellite orbits and an isothermal sphere Galactic potential, the halo extends to $\sim$210 kpc. Alternatively, if the rotation curve remains constant at the R_0 value of 220 km s^{-1}, the characteristic scale length of the halo is about 120 kpc.

c) *An Unbound Leo I?*

The above analyses are invalid if Leo I is not gravitationally bound to the Milky Way. If Leo I is unbound, then it probably has a place of origin other than the Milky Way, because at the observed velocity it would have traveled far beyond its current position in a Hubble time. The possible exception is that it was recently ejected from the Milky Way's system of satellites through a multibody encounter. However, none of the other satellites seems massive enough to have produced such an ejection. Another possible "birthplace" for Leo I is the M31 system. We have looked for orbits which would take Leo I near M31 when evolved backward in time.

If Leo I is unbound to the Milky Way, the data indicate that our Galaxy's mass is approximately $4 \times 10^{11}\ M_\odot$. If M31 is roughly twice as massive as the Milky Way, its mass is approximately $8 \times 10^{11}\ M_\odot$. In order that these masses and the Local Group mass inferred from the M31–Milky Way timing argument do not conflict, one must postulate that the Local Group has a dark matter component that is unassociated with either M31 or the Milky Way. To determine the mass in such a component we modeled it as a homogeneous sphere centered two-thirds of the way from the Milky Way to M31 which encompasses M31, the Milky Way, and Leo I. The positions of the Milky Way, with an adopted mass of $4 \times 10^{11}\ M_\odot$, and of M31, with an adopted mass of $8 \times 10^{11}\ M_\odot$, were evolved backward in time in a set of numerical simulations. For an age of the universe of 1.4×10^{10} yr, we determined that the necessary dark matter component (DMC) has a mass of $7.0 \times 10^{11}\ M_\odot$ interior to the position of the Milky Way.

To study the possible orbits of an unbound Leo I in such a Local Group, we ran a set of numerical simulations with M31, the Milky Way, and Leo I modeled as point masses, and the smooth DMC discussed above. Five thousand Leo I's were placed at the current spatial position with randomly chosen velocities that satisfy the following conditions: the radial component as viewed from the Milky Way is 177 km s^{-1}, and the total space velocity is less than 300 km s^{-1}. If the total space velocity exceeds 300 km s^{-1}, either the Leo I timing argument predicts a much larger mass for the Local Group than the M31–Milky Way–DMC timing argument, or Leo I is not bound to the Local Group (discussed below). The Leo I particles are influenced by the gravitational attraction of M31, of the Milky Way, and of the DMC. The particles representing Leo I, M31, and the Milky Way are evolved backward in time for 1.1×10^{10} yr by integrating Newton's equations of motion. The DMC experiences uniform expansion and contraction commensurate to that of M31 and the Milky Way. No Leo I test particle reached within 200 kpc of M31 during the simulation; therefore, we conclude that Leo I could not have originated in the M31 system.

In the model just described, Leo I is actually not bound to the Local Group; therefore, it cannot be a Local Group member which is unbound to the Milky Way. Since we have concluded that the place of origin of Leo I could not have been the M31 system, and since we have no viable model for the recent ejection of Leo I from the Milky Way's system of satellites, we must conclude that if this Local Group model is correct, Leo I originated outside the Local Group and is coincidentally passing by us. We cannot rule this possibility out, although it appears improbable. We conclude that the most reasonable assumption is that Leo I is bound to the Milky Way.

d) *Internal Velocity Dispersions*

The precision to which we have measured velocities in Leo I and II allows us to make some *preliminary* conclusions about the internal velocity dispersion of these systems and therefore about their M/L. Using the equations presented by Armadroff and Da Costa (1986), we derive that the internal velocity dispersions in Leo I and Leo II are 0.4 and 4 km s^{-1}, respectively. To estimate the largest velocity dispersion allowed by the data we assume that observational errors are negligible. For this

[5] The distance to Leo I quoted in the literature is simply based on the assignment of an absolute magnitude to the brightest red giants, or in the case of Fox and Pritchet (1987) on the assignment of $M_v = 0.6$ to a feature at the limit of their data which they identify as the horizontal branch. Both methods give distances in excess of 200 kpc. In addition, Aaronson and Mould (1985) measured infrared magnitudes for some of the stars discussed in this paper, as well as for others. Changing the adopted distance from 230 kpc to 150 kpc changes the distance modulus by 1 mag. As can be seen from Aaronson and Mould's (1985) Figures 3–5, a decrease of 1 mag for the bolometric magnitudes of these stars would make the abundances derived from IR photometry substantially larger than those measured by Suntzeff *et al.* (1986) from spectra of oxygen-rich giants. While an error in distance modulus of 0.5 mag (which drops the distance to 180 kpc) is not out of the question (for which the timing arguments suggest a Galactic mass $\geq 9 \times 10^{11}\ M_\odot$ for $t_0 = 1.4 \times 10^{10}$ yr), we believe that an error of 0.3 mag (which drops the distance to 200 kpc) is the largest reasonable error. Similarly, increasing the distance to Leo I makes the mass of the Galaxy even larger than proposed in this paper and also makes the derived abundances from IR photometry very low.

assumption the velocity dispersions in Leo I and II are 6 and 9 km s^{-1}, respectively.

The mass-to-light ratios for Leo I and II were obtained by assuming that a King model is a good approximation to their structure and deriving a mass using the equation

$$M = 167 r_c \mu \langle v_r^2 \rangle_0 \quad (8)$$

(Illingworth 1976), where r_c is the core radius in pc, μ depends on density structure and total mass and can be derived by fitting a particular model, and $(v_r)_0$ is the central radial velocity dispersion in km s^{-1}. For Leo I we adopt $r_c = 0.3$ kpc, $r_t = 0.91$ kpc, and an absolute magnitude of -11.4 (Hodge 1971). For Leo II we adopt $r_c = 0.2$ kpc, $r_t = 0.65$ kpc, and an absolute magnitude of -9.8 (Hodge 1971). The values of μ derived for the assumed parameters are 2.62 and 2.94 for Leo I and II, respectively, as derived from equations presented by King (1966). Using our upper limits for the velocity dispersions, we derive that M/L is ≤ 1.5 for Leo I and is ≤ 13 for Leo II, in solar units.

Our results for the M/L ratios support the claim of a relationship between M/L and absolute magnitude as discussed previously in the literature (e.g., Kormendy 1986). M/L ratio versus absolute magnitude are plotted for all the dwarf spheroidals in Figure 4. A determination of the cause of the trend will have important consequences for studies of dwarf galaxy formation and evolution. Because the observational errors are large compared to the estimated velocity dispersions, these results should be viewed as somewhat uncertain first estimates. We stress that the principal result is that these systems do not contain copious amounts of dark matter interior to r_c.

IV. CONCLUSIONS

The nature and distribution of dark matter in the universe is one of the most fundamental unanswered questions in astronomy. While the effects of dark matter have a tremendous impact on large-scale structure in the universe and on the basic nature and fate of the universe, it is relatively close to home where we find some of the most unambiguous evidence for its existence. It is with the sparsely populated dwarf spheroidal satellites of our own Galaxy that astronomers present a case for the ubiquitous presence of dark matter. The systemic velocities of these systems provide evidence for the presence of a large dark matter component in our Galaxy, and the internal velocity dispersion of stars in some of these systems provides evidence for a large dark matter component in the dwarf spheroidals themselves. We presented observations of the two most distant known dwarf spheroidal satellites, Leo I and II, and of two remote globular clusters, Eridanus and Pal 14, in order to extend and refine our knowledge of dark matter in our local neighborhood. In this paper we have done the following.

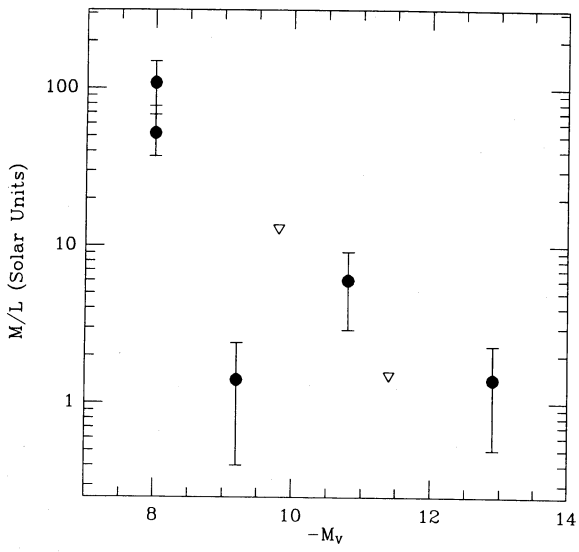

FIG. 4.—M/L vs. absolute magnitude for the dwarf spheroidal satellites of the Milky Way. The downward pointing triangles are upper limits and correspond to Leo I and II.

1. We demonstrated that etalon spectra can be used for accurate wavelength calibration across the entire observed spectral range. This technique allowed us to have a calibration spectral line every 7 to 10 Å. We attained velocity errors of 1/10th of a resolution element and feel that this could still be improved with optimized observing techniques. The method can be used in a number of applications.

2. We derived from measured velocities of three stars in Eridanus, two stars in Pal 14, six stars in Leo I, and five stars in Leo II that the heliocentric systemic velocities of these systems are -21 ± 4, 72 ± 4, 285 ± 3, and 70 ± 4 km s^{-1}, respectively. The values for Leo II, Eridanus, and Pal 14 are in agreement with some of the previously published values. The value for Leo I is in significant disagreement with the previous value.

3. We applied the analysis technique devised by Little and Tremaine (1987) to the enlarged data set. The large effect of Leo I on the results demonstrates how vulnerable this technique is to incompleteness, as well as to its assumptions about the eccentricity of orbits. Using LT's techniques we find the Galactic mass to be $M_G = 9.3^{+4.1}_{-1.2} \times 10^{11}\ M_\odot$ if satellite orbits are radial and $M_G = 12.5^{+8.4}_{-3.2} \times 10^{11}\ M_\odot$ if they are isotropic. These numbers assume a point source Galactic mass distribution. Our formal error estimates correspond to the 90% confidence level but the very dramatic effect of including or excluding one object, i.e., Leo I, demonstrates that this is a poor characterization of the true uncertainties. However, the results are in agreement within the errors with the lower limit obtained from timing arguments. We also conclude that while the isothermal sphere halo model appears to be more self-consistent the uncertainties in the orbital parameters of the remote systems lead to large uncertainties.

4. We used Leo I in classical timing arguments. These bypass certain weaknesses in the statistical analysis and lead to stringent constraints on the estimated mass of the Galaxy because of the uniquely large velocity and distance of this object. In our analysis we assumed purely radial orbits and point mass distributions, both of which lead to lower limits on the mass of the Galaxy. For our preferred model parameters, we estimate that the Galaxy has a mass of at least 13×10^{11} $M_\odot$. This is in excellent agreement with results from applying the timing argument to the orbit of M31 and the Milky Way (Kahn and Woltjer 1959; Einasto and Lynden-Bell 1982, and this paper), from an analysis of the Magellanic Stream which suggest $M_G \geq 8 \times 10^{11}\ M_\odot$ (Lin and Lynden Bell 1982), and with the mass required to bind the fastest local star, $M_G > 5 \times 10^{11}\ M_\odot$ (Carney, Latham, and Laird 1988). We conclude that $M_G = (13 \pm 2) \times 10^{11}\ M_\odot$, if Leo I has a radial orbit. If $v_c = 220$ km s^{-1} this implies that the halo extends to ~ 120 kpc.

5. We argued against the possibility that Leo I is not bound to the Milky Way. Using simple models of the Local Group,

which are consistent with the mass implied from the M31–Milky Way argument, we demonstrated that Leo I could not have originated in the M31 system. We also argue against a recent ejection of Leo I from the Milky Way system, against Local Group membership if it is unbound to the Milky Way, and against the coincidental passage of Leo I through the Local Group. We concluded that the most reasonable assumption is that Leo I is bound to the Milky Way.

6. We presented *preliminary* measurements of the internal velocity dispersions in Leo I and II, ≤ 6 and ≤ 9 km s^{-1}, respectively, and the corresponding mass-to-light ratios, ≤ 1.5 and ≤ 13, in solar units. The measured M/L ratios are in accordance with the trend of M/L with absolute magnitude seen in the other dwarf spheroidals. Our principal conclusion concerning M/L in these systems is that there is no evidence for a large (> 20) M/L.

Accurate and precise radial velocities are now available for all of the known remote systems; therefore, future improvements in the mass determination of our Galaxy will come primarily from improved knowledge of the nature of the orbits. Even with the rather crude determination of the Galactic mass presented here it is evident that our Galaxy has a large dark matter component, $\sim 10^{12}\ M_{\odot}$, and that the dark matter halo must extend to Galactocentric distances of ~ 100 kpc.

This work was partially supported by NSF grant AST 86-11405 to E. W. O. D. Z. acknowledges support from an NSF Graduate Fellowship. We thank John Hill for use of the cross-correlator software and Simon White for enlightening discussions from which this paper benefited substantially. R. A. S. thanks Steward Observatory and Peter Strittmatter for hospitality and partial support during his sabbatical visit there.

REFERENCES

Aaronson, M. 1983, *Ap. J. (Letters)*, **266**, L11.
Aaronson, M., and Mould, J. 1985, *Ap. J.*, **290**, 191.
Aaronson, M., and Olszewski, E. W. 1988, in *IAU Symposium 130, Large Scale Structures in the Universe*, ed. J. Audouze, M.-C. Pelletan, and A. Szalay (Dordrecht: Kluwer), p. 409.
Aaronson, M., Schommer, R. A., and Olszewski, E. W. 1984, *Ap. J.*, **276**, 221.
Aguilar, L., Hut, P., and Ostriker, J. P. 1988, *Ap. J.*, **335**, 720.
Allen, A. J., and Richstone, D. O. 1988, *Ap. J.*, **325**, 583.
Armandroff, T. E., and Da Costa, G. S. 1986, *A.J.*, **92**, 777.
Azzopardi, M., Lequeux, J., and Westerlund, B. E. 1985, *Astr. Ap.*, **144**, 388.
———. 1986, *Astr. Ap.*, **161**, 232.
Bontekoe, Tj. R., and van Albada, T. S. 1987, *M.N.R.A.S.*, **224**, 349.
Bosma, A. 1978, Ph.D. dissertation, University of Groningen.
Buonanno, R., Corsi, C. E., Fusi Pecci, F., Hardy, E., and Zinn, R. 1985, *Astr. Ap.*, **152**, 65.
Carney, B. W., Latham, D. W., and Laird, J. B. 1988, *A.J.*, **96**, 560.
Christian, C. A., and Heasley, J. N. 1986, *Ap. J.*, **303**, 216.
Cook, K., Schechter, P., and Aaronson, M. 1983, *Bull. AAS*, **15**, 907.
Da Costa, G. S. 1984, *Ap. J.*, **285**, 483.
———. 1985, *Ap. J.*, **291**, 230.
Da Costa, G. S., Ortolani, S., and Mould, J. 1982, *Ap. J.*, **257**, 633.
Da Costa, G. S., and Seitzer, P. O. 1989, preprint.
Dean, J. F., and Davies, R. D. 1975, *M.N.R.A.S.*, **170**, 503.
Delhaye, J. 1965, in *Stars and Stellar Systems, Galactic Structure*, Vol. **5**, ed. A. Blaauw and M. Schmidt (Chicago: University of Chicago Press), p. 61.
Demers, S., and Harris, W. E. 1983, *A.J.*, **88**, 329.
Einasto, J., and Lynden-Bell, D. 1982, *M.N.R.A.S.*, **199**, 67.
Foltz, C. B., Chaffee, F. H., Jr., Ouellette, D. B., and Blanco, D. R. 1985, MMT Technical Memo 85-4.
Fox, M. F., and Pritchet, C. J. 1987, *A.J.*, **93**, 1381.
Frenk, C. S., and White, S. D. M. 1982, *M.N.R.A.S.*, **198**, 173.
Godwin, P. J., and Lynden-Bell, D. 1987, *M.N.R.A.S.*, **229**, 7P.
Gratton, R. G., and Ortolani, S. 1984, *Astr. Ap. Suppl.*, **57**, 177.
Harris, W. E., and van den Bergh, S. 1984, *A.J.*, **89**, 1816.
Hartwick, F. D. A., and Sargent, W. L. W. 1978, *Ap. J.*, **221**, 512.
Hernandez, G. 1986, *Fabry-Perot Interferometers* (Cambridge: Cambridge University Press).
Hodge, P. W. 1971, *Ann. Rev. Astr. Ap.*, **9**, 35.
Illingworth, G. 1976, *Ap. J.*, **204**, 73.
Kahn, F. D., and Woltjer, L. 1959, *Ap. J.*, **130**, 705.
Kent, S. M. 1988, *A.J.*, **96**, 514.
King, I. R. 1966, *A.J.*, 71, 64.
Kormendy, J. 1986, in *IAU Symposium 117, Dark Matter in the Universe*, ed. J. Kormendy and G. Knapp (Dordrecht: Reidel), p. 139.
Lin, D. N. C., and Lynden-Bell, D. 1982, *M.N.R.A.S.*, **198**, 707.
Little, B., and Tremaine, S. 1987, *Ap. J.*, **320**, 493 (LT).
Lynden-Bell, D., Cannon, R. D., and Godwin, P. J. 1983, *M.N.R.A.S.*, **204**, 87P (LCG).
Mathieu, R. D., Latham, D. W., Griffin, R. F., and Gunn, J. E. 1986, *A.J.*, **92**, 1110.
McGlynn, T. A. 1984, *Ap. J.*, **281**, 13.
Mould, J., and Aaronson, M. 1983, *Ap. J.*, **273**, 530.
Olszewski, E. W., and Aaronson, M. 1985, *A.J.*, **90**, 2221.
Olszewski, E. W., Peterson, R. C., and Aaronson, M. 1986, *Ap. J. (Letters)*, **302**, L45 (OPA).
Peterson, R. C. 1985, *Ap. J.*, **297**, 309.
Peterson, R. C., and Foltz, C. B. 1986, *Ap. J.*, **307**, 143.
Peterson, R. C., and Latham, D. W. 1989, *Ap. J.*, **336**, 178 (PL).
Peterson, R. C., Olszewski, E. W., and Aaronson, M. 1986, *Ap. J.*, **307**, 139.
Pike, C. D. 1976, *M.N.R.A.S.*, **177**, 257.
Pryor, C. P., Latham, D. W., and Hazen, M. L. 1988, *A.J.*, **96**, 123.
Racine, R., and Harris, W. E. 1975, *Ap. J.*, **196**, 413.
Rubin, V. C., Ford, W. K., Jr., Thonnard, N., and Burstein, D. 1982, *Ap. J.*, **261**, 439.
Sandage, A. 1986, *Ap. J.*, **307**, 1.
Sandage, A., Katem, B., and Johnson, H. L. 1977, *A.J.*, **82**, 389.
Schommer, R. A., Olszewski, E. W., and Aaronson, M. 1984, *Ap. J. (Letters)*, **285**, L53.
Schweizer, L. Y. 1987, *Ap. J. Suppl.*, **64**, 427.
Seitzer, P. O., and Carney, B. W. 1988, preprint.
Seitzer, P. and Frogel, J. A. 1985, *A.J.*, **90**, 1796.
Stetson, P. B. 1979, *A.J.*, **84**, 1149.
Suntzeff, N. B., Aaronson, M., Olszewski, E. W., and Cook, K. H. 1986, *A.J.*, **91**, 1091.
Suntzeff, N., Olszewski, E., and Stetson, P. B. 1985, *A.J.*, **90**, 1481.
Tonry, J., and Davis, M. 1979, *A.J.*, **84**, 1511.
van Albada, T. S. 1982, *M.N.R.A.S.*, **201**, 939.
van den Bergh, S. 1980, in *The Structure and Evolution of Normal Galaxies*, ed. S. M. Fall and D. Lynden-Bell (Cambridge: Cambridge University Press), p. 201.
Webbink, R. F. 1985, *IAU Colloquium 113, Dynamics of Star Clusters*, ed. J. Goodman and P. Hut (Dordrecht: Reidel), p. 541.
Welch, D. L., McAlary, C. W., McLaren, R. A., and Madore, B. F. 1986, *Ap. J.*, **305**, 583.
White, S. D. M., Huchra, J., Latham, D., and Davis, M. 1983, *M.N.R.A.S.*, **203**, 701.
Yahil, A., Tammann, G. A., and Sandage, A. 1977, *Ap. J.*, **217**, 903.
Zaritsky, D. and White, S. D. M. 1989, in preparation.

MARC AARONSON, EDWARD W. OLSZEWSKI, and DENNIS ZARITSKY: Steward Observatory, University of Arizona, Tucson, AZ 85721

RUTH C. PETERSON: Whipple Observatory, Smithsonian Institution, Steward Observatory Offices, University of Arizona, Tucson, AZ 85721

ROBERT A. SCHOMMER: Department of Physics and Astronomy, Serin Physics Laboratory, P.O. Box 849, Rutgers University, Piscataway, NJ 08855-0849